Biochemistry

 Volume 29, Number 8 February 27, 1990

Accelerated Publications

500-Picosecond Molecular Dynamics in Water of the Manα1→2Manα Glycosidic Linkage Present in Asn-Linked Oligomannose-Type Structures on Glycoproteins†

C. J. Edge,‡ U. C. Singh,§ R. Bazzo,‡ G. L. Taylor,‖ R. A. Dwek,‡ and T. W. Rademacher*,‡

Oxford Glycobiology Unit, Department of Biochemistry, and Department of Molecular Biophysics, University of Oxford, South Parks Road, Oxford OX1 3QU, U.K., and Scripps Clinic and Research Foundation, MB19, 10666 North Torrey Pines Road, La Jolla, California 92037

Received October 31, 1989; Revised Manuscript Received December 7, 1989

ABSTRACT: Molecular dynamics simulations of the Manα1→2Manα glycosidic linkage found in the N-linked glycans of glycoproteins were performed in vacuo and in the presence of water. In the latter case significant dampening of the molecular fluctuations was found when compared to the in vacuo simulation. A 500-ps dynamics simulation in water showed only occasional short-lived deviations from the minimum-energy conformation, more consistent with carbohydrate "breathing" than flexibility. These studies add further evidence that oligosaccharides can maintain "fixed" geometries with relatively long lifetimes and are in agreement with experimental NMR-derived parameters for the same linkage in oligomannose structures.

Molecular dynamics is a well-established method for the investigation of the conformational behavior of the protein part of glycoproteins and DNA [McCammon et al. (1987) and references cited therein]. These studies have been conducted both in vacuo and in various solvents and have contributed greatly to the understanding of the exact nature of the substantial structural fluctuations that may occur in such molecules. Experimentally, such fluctuations have been shown to be essential for biological activity (Artymiuk, 1988).

Until recently, little attention has been focused on an important structural component of glycoproteins, namely, the oligosaccharides attached to the protein molecule. Much experimental evidence has been put forward to show that the oligosaccharide moieties on a glycoprotein may play a fundamental role in regulating the biological activity of a protein (Rademacher et al., 1988). Indeed, a given glycoprotein may be represented in the organism as several different *glycoforms* (the same protein with different oligosaccharides at the sugar attachment sites). The prevalence of each glycoform may be influenced by the age and physiological status of the organism, including a number of disease states.

The question as to how an oligosaccharide can span its conformational space and influence the functionality of its parent protein can be resolved with molecular dynamics. Previous computer simulations of similar compounds have been performed in vacuo with a variety of force fields, some of which have attempted to include the effect of water implicitly in the parameterization (Brady, 1986, 1987; Homans et al., 1987). In this paper, the AMBER (Weiner et al., 1984) force field, previously developed for proteins and nucleic acids, is adapted for carbohydrates. The force field is then applied to the disaccharide mannose-α1→2-mannose-α, which is present in the outer arms of the oligomannose-type oligosaccharides (Figure 1). The results from running a 500-ps simulation of the disaccharide in water solvent are then compared with the average conformation for this disaccharide obtained from nuclear magnetic resonance (NMR) data from compound II (Homans et al., 1987).

Materials and Methods

Potential Energy Surface. The molecule Manα1→2Manα was constructed with the INSIGHT graphics package (Biosym Technologies Inc., San Diego, CA) and the structure minimized to a low energy with the AM1 Hamiltonian of the AMPAC (Dewar et al., 1986) molecular orbital package. This structure and the partial charges obtained from a Mullikan

† The Oxford Glycobiology Unit is supported by Monsanto. U.C.S. acknowledges support from NIH Research Grants GH39310 and GH38784.

‡ Oxford Glycobiology Unit, Department of Biochemistry, University of Oxford.

§ Scripps Clinic and Research Foundation.

‖ Department of Molecular Biophysics, University of Oxford.

0006-2960/90/0429-1971$02.50/0

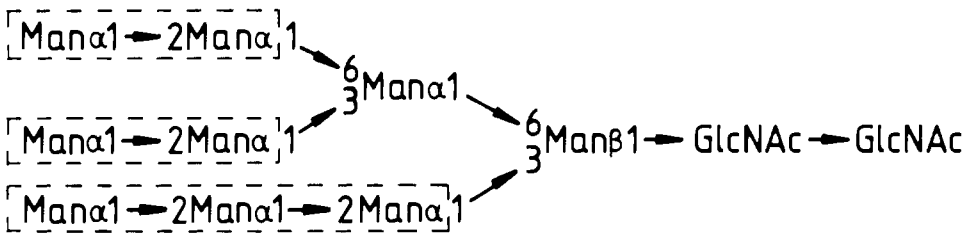

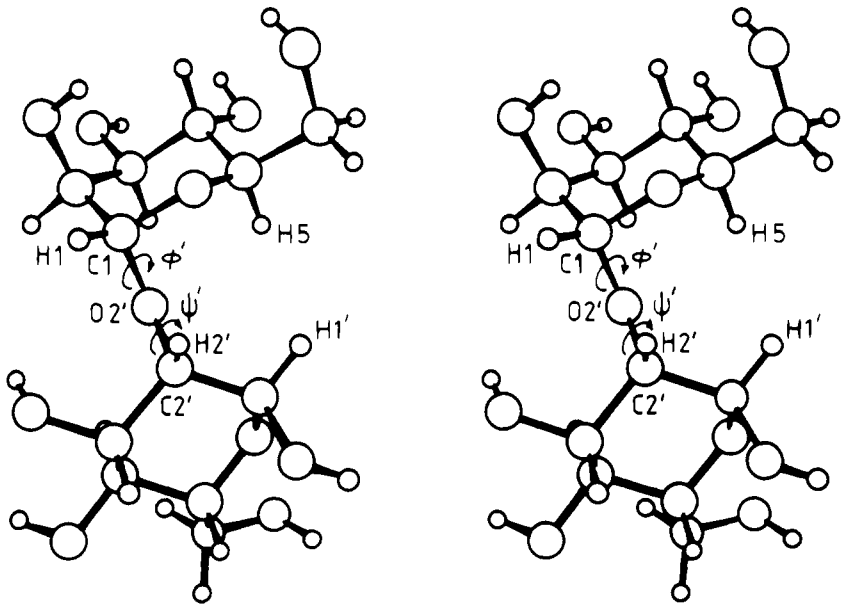

FIGURE 1: (Top) The oligomannose structure, $Man_9GlcNAc_2$, contains four Manα1–2Manα linkages present in the outer arms (boxes). (Bottom) The energy-minimized conformation of Manα1–2Manα, not including the 545 water molecules, in stereo. The atoms are labeled as explained in the text. The torsion angles ϕ' and ψ' are shown.

Table I: Values of V_n and γ_n for Torsional Linkage H1–C1–O1–HO1

n	$V_n/2$ (kcal/mol)	γ_n (deg)
1	1.56	77.58
2	0.48	110.03
3	0.31	358.01
4	−0.16	41.81
5	−0.16	359.75

Table II: Values of V_n and γ_n for Torsional Linkage H2–C2–O2–HO2

n	$V_n/2$ (kcal/mol)	γ_n (deg)
1	1.07	34.90
2	1.38	112.02
3	0.37	294.40
4	−0.71	38.62
5	−0.17	0.00

population analysis carried out on the structure were used in subsequent molecular mechanics and dynamics calculations. The angles ϕ' (defined as H1–C1–O2′–C2′, with the prime present to distinguish it from IUPAC notation) and ψ' (defined as C1–O2′–C2′–H2′) were independently varied over the range −180° to 180° in steps of 30° and the resultant 144 structures minimized with AMBER as described in the legend to Figure 2 with the parameters for the torsion angles H1–C1–O2′–C2′ and C1–O2′–C2′–H2′ the same as those calculated for H1–C1–O1–HO1 and H2–C2–O2–HO2, respectively (see Figure 1 for labeling of the angles ϕ' and ψ').

By use of the set of functions given in the legend to Figure 2, values of V_n [barrier height (kcal/mol)] and γ_n [phase (degrees)] for the torsional linkage H1–C1–O1–HO1 were obtained and are presented in Table I while those for the linkage H2–C2–O2–HO2 are presented in Table II. The potential energy surface that results from plotting the energies at 144 different ϕ', ψ' values for Manα1→2Manα is shown in Figure 2. On this surface there is a single deep minimum at a value of $\phi' = -60°$, $\psi' = 0°$. This energy surface agreed well in qualitative terms with a previous energy surface calculated for the Manα1→2Manα disaccharide (Homans et al., 1987).

Molecular Dynamics Simulations. Molecular dynamics simulations on Manα1→2Manα were carried out on the above potential energy surface with the NEWTON module of the AMBER package [Version 3.1 is a fully vectorized and parallelized version of AMBER (3.0) by Singh et al. (1986)]. All atoms were treated explicitly (all-atom force field). The initial energy configuration from AMPAC was immersed in a box of 545 TIP3P water molecules. This was minimized within the AMBER force field with a dielectric constant of 1 and a cutoff value for the nonbonded pair interactions of 8.0 Å. The resulting structure (Figure 1) was used as the starting configuration for the dynamics simulation. Initial velocities for the atoms were selected from a Maxwellian distribution at 10 K, and the system was coupled to a thermal bath with a coupling constant $\tau = 0.4$ ps^{-1}. The dielectric constant was again 1 with a nonbonded cutoff distance of 8.0 Å and a time step of 0.1 fs. The simulation was performed under a constant pressure of 1 atm and allowed to equilibrate to a temperature of 300 K for 20 ps, when it was found that the root mean square temperature fluctuation was ±2 K. A further 30 ps of dynamics was then run and analyzed with a Convex C210 processor.

Comparison to NMR Results. It was decided to investigate whether use of the SHAKE algorithm (Ryckaert et al., 1977), which is used to constrain all bond lengths to their equilibrium

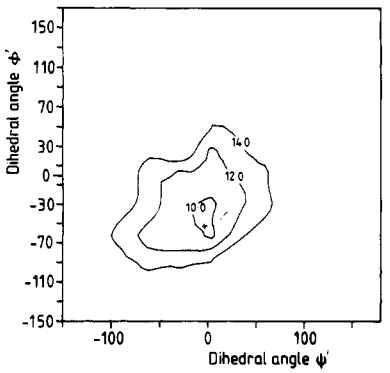

FIGURE 2: Potential surface generated with AMBER including the parameters from Tables I and II. The energy levels are shown in kcal/mol. The symbol (+) shows the minimum-energy position on the surface. Complete optimization of bond lengths, bond angles, and torsion angles was carried out on the coordinates from the crystal structure of α-mannose with the AM1 Hamiltonian in the AMPAC molecular orbital package (Dewar et al., 1986). The optimization was performed on a Floating Point Systems M64/30 computer. Ring carbon atoms were labeled clockwise C1 to C5, with C1 as the anomeric carbon atom as shown in Figure 1. The ring oxygen was designated as O5. The remaining oxygen and hydrogen atoms directly attached to carbon were labeled according to their parent carbon atoms, with hydroxyl hydrogens being labeled HOX (X is the number of the parent oxygen atom). The torsional angles ϕ = H2–C2–O2–HO2 and ϕ = H1–C1–O1–HO1 were varied individually in steps of 30° ($-180° < \phi \leq 180°$). The energy of the structures was calculated, allowing the rest of the bond lengths, bond angles, and torsional angles to be optimized, with the AM1 Hamiltonian in the AMPAC package. The 24 resultant structures (12 from each torsion analysis) and their corresponding energies were then saved and used in the molecular mechanics analysis below. The molecular mechanics force field chosen in this study was AMBER since the force field contains the term $\sum V_\eta[1 + \cos(\eta\theta - \gamma_\eta)]/2$ (η = 1,6) (eq 1), where V_η is the barrier height, θ is the torsional angle, and γ_η is the phase. Using this term, it was possible to fit complex periodic functions such as are observed in the variation of energy with ϕ rotation in a given monosaccharide. The 24 structures from the AMPAC calculations were then minimized with AMBER with the important proviso that, in the standard AMBER all-atom parameter file, the parameters for the dihedral angle ϕ being examined at the time were set to zero. The partial charges used in the AMBER minimization were those calculated from a Mullikan population analysis performed by the AMPAC program. For each set of AMPAC torsional angle calculations the minimum energy was found and subtracted from the other energy values. The procedure was repeated for the two sets of AMBER energy values. The resultant AMBER values were then subtracted from the AMPAC values: $\xi_\phi = (E_\phi^{AMPAC} - E_0^{AMPAC}) - (E_\phi^{AMBER} - E_0^{AMBER})$. The function ξ_ϕ was plotted against ϕ and fitted to the AMBER torsional terms in eq 1 with a nonlinear least-squares fitting program.

distance, had any effect on the variation of the torsional angles ϕ' and ψ' and whether the simulation would be able to reproduce the results obtained from NMR studies on various oligomannose compounds in terms of the interproton distances across the glycosidic linkage obtained from nuclear Overhauser effect (NOE) data (Noggle et al., 1971). Accordingly, the minimized starting structure was taken and equilibrated with the SHAKE algorithm with a time step of 2 fs for 20 ps. The dielectric constant and nonbonded cutoff were set to the same values as before. A further 500 ps of dynamics was then run and analyzed on a single-processor Cray-XMP supercomputer. Comparison of the simulations in water was carried out with a simulation in vacuo. The Manα1→2Manα molecule was constructed as before, and the atoms were given the same partial charges. With use of a dielectric constant of 50 to simulate the presence of solvent, a nonbonded cutoff of 12.0 Å, and a time step of 0.1 fs, the disaccharide was equilibrated for 20 ps. A further 30 ps of simulation was then carried out, and the results were analyzed. The SHAKE algorithm was not used during this simulation.

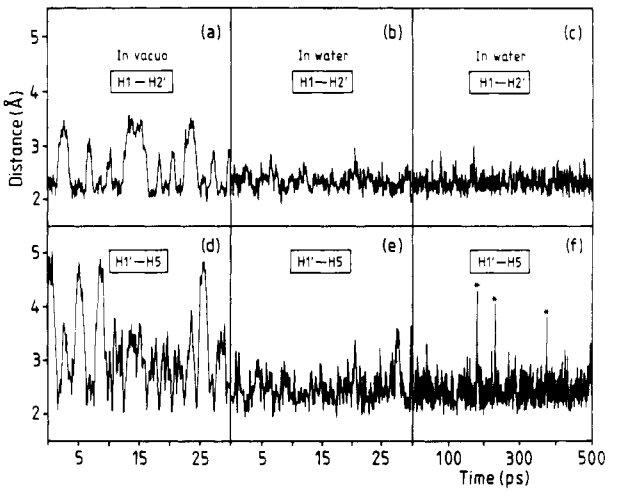

FIGURE 3: Plots of interproton distances H1–H2′ and H1′–H5 versus time. Panels a and d show the results of the 30-ps simulation in vacuo while panels b and e show the results for the 30-ps simulation in water. 500-ps plots of interproton distances for H1–H2′ and H1′–H5 versus time are shown in panels c and f, respectively.

Table III: Average Distances and Standard Deviations Calculated for Two Atom Pairs from the Three Molecular Dynamics Simulations[a]

	atom pairs	$\langle r_{ij} \rangle$	SD	$\langle r_{ij} \rangle$ virtual
30-ps in vacuo simulation	H1–H2′	2.55	0.44	2.36
	H1′–H5	3.13	0.73	2.70
30-ps water simulation without SHAKE	H1–H2′	2.33	0.16	2.29
	H1′–H5	2.48	0.31	2.37
500-ps water simulation using SHAKE	H1–H2′	2.31	0.16	2.28
	H1′–H5	2.45	0.29	2.36
NMR results	H1–H2′			2.33 ± 0.1
	H1′–H5			2.53 ± 0.1

[a] These are compared with the virtual distances calculated from the averaged NOEs and with the NMR results from Homans et al. (1987), assuming the linear NOE buildup approximation.

RESULTS

Comparison of the in vacuo and the water simulations shows that the disaccharide, during the in vacuo simulation, spends more time at larger interproton distances. In Figure 3 it is seen that the in vacuo simulation interproton distance H5–H1′ often becomes as large as 5 Å, while the "normal" range of motion is between 2.0 and 3.5 Å. This must be compared with the water simulation of the H5–H1′ interproton distance where the fluctuations are between 2.0 and 3.0 Å with an occasional increase to 3.6 Å. Over a longer period of time (500 ps) there are occasional large fluctuations to 4.2 Å, but it appears that the presence of solvent prevents any fluctuations as far as 5.0 Å from occurring (Figure 3). Similar remarks may be made about the H1–H2′ interproton distance in vacuo and in solvent. Further, there are no great differences seen between the simulations where the SHAKE algorithm was used and where it was omitted.

For each simulation, a theoretical set of NOEs (assuming a mixing time of 250 ms and a correlation time in the experimental range) were calculated with the relaxation matrix approach (Noggle & Schirmer, 1971), and the NOE values were averaged over the dynamics runs. In Table III the actual averaged distances for two atom pairs are compared with the virtual distances calculated from the average NOEs and with the NMR results derived in Homans et al. (1987), assuming the linear NOE buildup approximation. The agreement is good, if we consider the estimated experimental error. However, in this example we observe that the assumption of a fixed

conformation introduces a more significant discrepancy than the linear buildup approximation.

The torsional rotation of any given hydroxyl group in a given monosaccharide is a complex function of the torsional rotation angle ϕ about the C–O bond. The complexity is due to steric terms and Coulombic terms, making it impossible to describe the rotation in a simple way. In this paper, the use of rather complex torsional parameters has allowed the torsional rotation of the 2-OH and 1-OH groups to be addressed in the disaccharide Manα1→2Manα. Further, it has been shown that, by obtaining the correct torsional parameters for the 1-OH and 2-OH groups, the terms for the monosaccharides can be added together to produce an energy surface that gives good agreement with NMR experimental results when molecular dynamics simulations are run on it. For simple glycosidic linkages, e.g., 1→2, 1→3, and 1→4, it would appear to be unnecessary to include cross-correlational torsion terms, but this may not be the case for the 1→6 linkage where ω (the torsional rotation about the C5–C6 bond) depends on ϕ (the torsional rotation about the C6–O6 bond).

The simulation in vacuo of Manα1→2Manα disaccharide shows that there is much more oscillation about the glycosidic linkage than if the simulation is run in solvent. In vacuo the molecule spends more of its time in a configuration that is less likely to be observed, according to the NMR NOE data. Addition of solvent, however, restricts the oscillation about the glycosidic linkage to be more consistent with experimental values. There are, however, several occasions during the 500-ps simulation when the conformation of the Manα1→2Manα linkage deviates markedly from the minimum-energy conformation. These configurations are so short lived (of the order of 1 ps) that it is unlikely that they will contribute significantly to the range of conformations that is responsible for the binding of Manα1→2Manα to various ligands.

Discussion

An understanding of the conformational preferences and the lifetimes (dynamics) of individual oligosaccharide conformers is critical to our understanding of the biosynthesis of oligosaccharides and to the way oligosaccharides interact with their "host" proteins. The biosynthesis of oligosaccharides while covalently attached to folded peptide domains is not template driven but appears to be controlled in part by polypeptide–oligosaccharide interactions, which stabilize particular oligosaccharide conformers. Recognition of, or failure to interact with, specific oligosaccharide conformers by processing enzymes (exoglycosidases, glycosyltransferases) continues or diverges the biosynthetic pathway.

A carbohydrate primarily interacts with the protein to which it is attached to up- or downregulate its activity; i.e., there is an interactive relationship between the peptide and its attached oligosaccharide, which is formed as a consequence of the mechanism of oligosaccharide biosynthesis. For example, the addition of O-linked carbohydrate side chains (attached to Ser/Thr) has recently been shown to reduce the mobility of the glycosylated residues by nearly an order of magnitude. Mucins have also been proposed to have a highly expanded conformation that is dominated by steric interactions between the peptide core and the O-linked GalNAc residues (Gerken et al., 1989). Similarly, we have recently shown that in N-linked glycans the GlcNAc-Asn linkage is rigid, and therefore, the conformational space available to the oligosaccharide will depend to a large extent upon the mobility of the Asn side chain (Wooten et al., 1989). Although at present long-range interactions have not been experimentally confirmed, the differential positioning of the Asn side chain due to local protein secondary structures could increase or decrease the degree of interaction of the oligosaccharide with the protein. This in turn creates unique microenvironments that could be the basis for site-specific oligosaccharide biosynthesis. Further, this mechanism allows for oligosaccharide surfaces to be formed on those glycoproteins containing multiple glycosylation sites.

Finally, future molecular dynamics studies on the α1→3 and α1→6 linkages, which may have more than one conformational minimum, should lead to a more meaningful description of oligosaccharide three-dimensional structure than our present static concept.

Acknowledgments

We thank Dr. Richard A. Lerner for providing access to the supercomputer facility at Scripps Clinic for part of this work.

Supplementary Material Available

Table listing AMPAC-derived parameters for Manα1→2Manα in the minimum-energy configuration, including atom name, bond length, bond angle, dihedral angle, *Z* matrix, and partial charges (1 page). Ordering information is given on any current masthead page.

References

Artymiuk, P. (1988) *Nature 332*, 582.
Brady, J. W. (1986) *J. Am. Chem. Soc. 108*, 8153–8160.
Brady, J. W. (1987) *Carbohydr. Res. 165*, 306–312.
Dewar, M. J. S., & Stewart, J. J. P. (1986) AMPAC, *QCPE Bull. 506*.
Gerken, T. A., Butenhof, K. J., & Shogren, R. (1989) *Biochemistry 28*, 5536–5543.
Homans, S. W., Pastore, A., Dwek, R. A., & Rademacher, T. W. (1987) *Biochemistry 26*, 6649–6655.
McCammon, J. A., & Harvey, S. C. (1987) *Dynamics of Proteins & Nucleic Acids*, Cambridge University Press, Cambridge.
Noggle, J. H., & Schirmer, R. E. (1971) in *The Nuclear Overhauser Effect*, Academic Press, New York.
Rademacher, T. W., Parekh, R. B., & Dwek, R. A. (1988) *Annu. Rev. Biochem. 57*, 785–383.
Ryckaert, J. P., Cicotti, G., & Berendsen, H. J. C. (1977) *J. Comput. Phys. 23*, 327–341.
Singh, U. C., Weiner, P. K. Caldwell, J. W., & Kollman, P. A. (1986) Version 3.1, University of California, San Francisco.
Weiner, S. J., Kollman, P. A., Case, D. A., Singh, U. C., Ghio, C., et al. (1984) *J. Am. Chem. Soc. 106*, 765–784.
Wooten, E. W., Dwek, R. A. Feinstein, A., & Rademacher, T. W. (1989) Structural Features of the Tailpiece from Serum IgM and Their Implications for Oligosaccharide-Protein Interactions (submitted for publication).